

A Mammalian Iron ATPase Induced by Iron*

Received for publication, December 9, 1999, and in revised form, February 3, 2000

David E. Barañano[‡], Herman Wolosker^{‡§}, Byoung-II Bae[‡], Roxanne K. Barrow[‡],
Solomon H. Snyder^{‡¶}, and Christopher D. Ferris^{‡**‡‡}

From the Departments of [‡]Neuroscience, [¶]Pharmacology and Molecular Sciences, and ^{||}Psychiatry and Behavioral Sciences, and Department of ^{**}Medicine, Division of Gastroenterology, The Johns Hopkins University School of Medicine, Baltimore, Maryland 21205

While molecular mechanisms for iron entry and storage within cells have been elucidated, no system to mediate iron efflux has been heretofore identified. We now describe an ATP requiring iron transporter in mammalian cells. ⁵⁵Fe is transported into microsomal vesicles in a Mg-ATP-dependent fashion. The transporter is specific for ferrous iron, is temperature- and time-dependent, and detected only with hydrolyzable nucleotides. It differs from all known ATPases and appears to be a P-type ATPase. The Fe-ATPase is localized together with heme oxygenase-1 to microsomal membranes with both proteins greatly enriched in the spleen. Iron treatment markedly induces ATP-dependent iron transport in RAW 264.7 macrophage cells with an initial phase that is resistant to cycloheximide and actinomycin D and a later phase that is inhibited by these agents. Iron release, elicited in intact rats by glycerol-induced rhabdomyolysis, induces ATP-dependent iron transport in the kidney. Mice with genomic deletion of heme oxygenase-1 have selective tissue iron accumulation and display augmented ATP-dependent iron transport in those tissues that accumulate iron.

Living cells require iron for many critical biological functions, including cellular respiration and DNA synthesis. Iron's physiologic importance derives from its ability to exist in multiple valence states and therefore participate in reactions requiring single electron transfers. Pathophysiologically, electron transfer by iron can generate toxic free radicals, such as the hydroxyl radical (1, 2). Various mechanisms regulate cellular iron to ensure adequate supplies for cellular physiology while avoiding toxic iron excess.

Many of the molecular details for iron accumulation and storage in cells are known. Iron circulates in the blood in the ferric form (Fe³⁺) bound tightly to transferrin (3, 4). In most physiologic situations, iron enters cells upon the binding of diferric transferrin to the transferrin receptor followed by receptor-mediated endocytosis. Acidification of the lumen of the endocytic vesicle by the H⁺-ATPase releases iron from transferrin, whereupon iron is transported into the cytoplasm by the divalent cation transporter (5). Excess cellular iron can be stored by ferritin (4). Transferrin receptor and ferritin levels

are reciprocally controlled by iron regulatory proteins (IRPs)¹ that bind to specific sequences known as iron regulatory elements (IREs) in the mRNAs of these proteins (3, 4, 6, 7).

In contrast, molecular details of a cellular iron efflux pathway are lacking, even though physiologic evidence indicates that bodily stores of iron are conserved and re-utilized. Thus, the human daily dietary requirement for iron is only 1 mg, despite evidence that tissues mobilize 20–30 times that amount to support red blood cell synthesis by the bone marrow (8). Iron is released from hemoglobin and other heme proteins by heme oxygenase-1 (HO1), an inducible enzyme associated with the endoplasmic reticulum, which cleaves the heme ring giving rise to biliverdin, which is rapidly reduced to bilirubin, carbon monoxide, and ferrous iron (9). In mice with targeted genomic deletion of HO1, tissue stores of iron are elevated, while serum iron levels are low (10, 11). Recently, we demonstrated that expression of HO1 is linked to cellular iron efflux, demonstrating a role for HO1 in cellular iron mobilization (12).

Since HO1 is an enzyme that catalyzes the breakdown of cytosolic heme but is not a transport protein, the mechanism by which HO1 activity is linked to cellular iron mobilization remains obscure. We reasoned that a membrane-associated transporter, like the calcium ATPase, might be the molecular link between cytosolic heme catabolism by HO1 and cellular iron release. We now report the identification and characterization of an Fe-ATPase associated with microsomal membranes that is co-distributed in tissues with HO1. Iron induces ATP-dependent iron transport in a macrophage cell line and in HO1^{-/-} mice, and glycerol-induced rhabdomyolysis induces ATP-dependent iron transport in the kidney.

EXPERIMENTAL PROCEDURES

Materials—⁵⁵FeCl₃ (39.7 Ci/g) was obtained from NEN Life Science Products and used without altering the specific activity. Unless otherwise indicated all other chemicals were from Sigma.

Microsome Preparation—For routine isolation of microsomes all manipulations were performed at 4 °C as follows. Tissues or cell cultures were harvested and homogenized with 15 strokes of a Dounce-Teflon homogenizer in five volumes of ice-cold homogenization buffer (0.28 M sucrose, 20 mM Hepes (pH 7.5), 2 mM β-mercaptoethanol, protease inhibitors). The homogenate was centrifuged at 20,000 × g for 15 min to remove intact cells, nuclei, mitochondria, and other debris. The resulting supernatant was then centrifuged at 200,000 × g for 45 min to isolate the microsomal fraction. This second pellet was resuspended in homogenization buffer at a concentration of approximately 20 mg/ml protein, and samples were stored at –80 °C for up to one month prior to use.

Differential Centrifugation—Spleen tissue was homogenized as described above, and the homogenate was centrifuged at 1000 × g for 20

* This work was supported by United States Public Health Service Grant MH-18501 and Research Scientist Awards DA-00074 (to S. H. S.) and DA-05900 (to D. E. B.). The costs of publication of this article were defrayed in part by the payment of page charges. This article must therefore be hereby marked "advertisement" in accordance with 18 U.S.C. Section 1734 solely to indicate this fact.

§ Present address: Dept. de Bioquímica Médica, ICB/CCS, Universidade Federal do Rio de Janeiro, Rio de Janeiro 21941–590, Brazil.

‡‡ Howard Hughes Fellowship for Physicians. To whom correspondence should be addressed. Tel.: 410-955-2380; Fax: 410-955-3623; E-mail: cferris@jhmi.edu.

¹ The abbreviations used are: IRP, iron regulatory protein; IRE, iron regulatory element; HO1, heme oxygenase-1; HO2, heme oxygenase-2; AD, actinomycin D; CHX, cycloheximide; ER, endoplasmic reticulum; ATP_γS, adenosine 5'-(thiotriphosphate); AMP-PCP, adenosine 5'-(β,γ-methylenetriphosphate); AMP-PNP, adenosine 5'-(β,γ-iminotriphosphate).

min. The resulting pellet (P1), containing nuclei, intact cells, and debris, was resuspended in ice-cold homogenization buffer at a concentration of ~ 20 mg/ml protein and stored at -80°C prior to use. The first supernatant (S1) was centrifuged at $10,000 \times g$ for 15 min. The resulting pellet (P2), containing mitochondria, was likewise resuspended in homogenization buffer (~ 20 mg/ml protein) and stored (-80°C). The second supernatant (S2) was centrifuged at $200,000 \times g$ for 45 min. This pellet (P3) was also resuspended in homogenization buffer (~ 20 mg/ml protein) and stored (-80°C). Marker enzymes for specific subcellular organelles were assayed as described previously (13).

ATP-dependent Iron Transport Assay—For routine experiments, microsomes were thawed on ice, aliquoted ($10\text{--}100 \mu\text{g}$ of protein) into reaction buffer (140 mM potassium gluconate, 40 mM Hepes (pH 7.5), 2 mM ascorbate, 5 mM MgSO_4 , 4 mM Na_2ATP , and $5 \mu\text{M}$ $^{55}\text{FeCl}_3$) in a final volume of $115 \mu\text{l}$ and incubated at 30°C . At the indicated times, $100 \mu\text{l}$ of this reaction mixture was rapidly filtered (vacuum manifold, $0.45\text{-}\mu\text{m}$ filter, Millipore) and washed under continuous vacuum with 25 ml of ice-cold wash buffer (140 mM potassium gluconate, 20 mM Hepes (pH 7.5)). ^{55}Fe associated with the filters was determined by liquid scintillation spectrometry. In routine experiments, a similar reaction without ATP was used to determine nonspecific iron accumulation. Unless otherwise indicated, zero time was defined as the time when the microsomes were added to the reaction buffer. When iron transport was measured in the presence of other ions, the chloride salt of the corresponding ion was included in the reaction buffer with the $^{55}\text{FeCl}_3$, before the microsomes were added. All reactions were prepared and measured in duplicate or triplicate as indicated in the figure legends.

Cell Culture—RAW 264.7 cells were cultured in Dulbecco's modified Eagle's medium (Life Technologies, Inc.) supplemented with 10% fetal bovine serum, penicillin and streptomycin, and glutamine using standard techniques (14). Briefly, RAW 264.7 cells were maintained in continuous culture, changing the medium every 2–3 days, for no more than

4 weeks. When cultures reached $>90\%$ confluence, they were subcultured at a ratio of 1:5 for use in experiments or to carry the line. Unless otherwise indicated, experiments were performed when cells were approximately 90% confluent. Iron treatment of RAW 264.7 cells was performed by including 0.5 mM FeSO_4 in the medium for various times as indicated in the figures. In some experiments actinomycin D ($1 \mu\text{g/ml}$) or cycloheximide ($100 \mu\text{g/ml}$) was added as described in the figure legend to Fig. 5B to block transcription and translation respectively.

Western Blot Analysis—HO1 and heme oxygenase-2 (HO2) expression were analyzed by Western blot analysis using antibodies developed

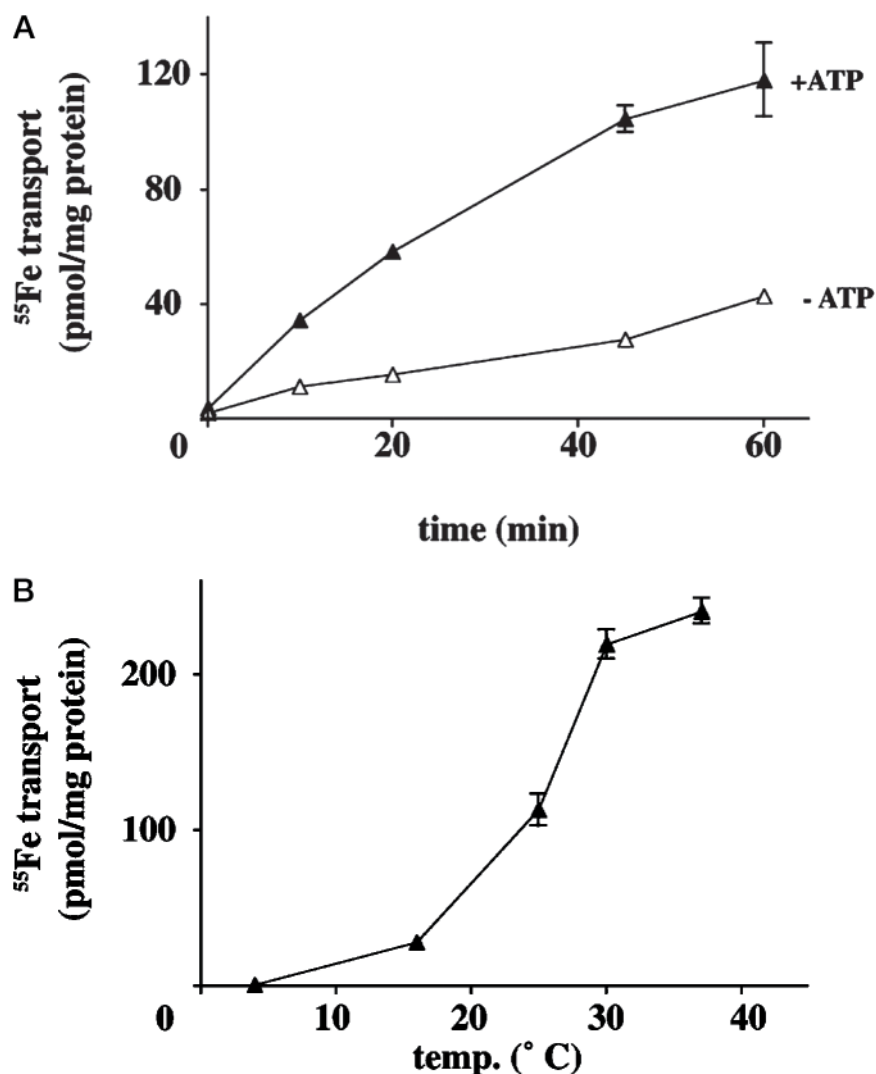
TABLE I

Nucleotide specificity of ^{55}Fe accumulation in spleen microsomes

Spleen microsomes were prepared as described under "Experimental Procedures" and incubated for 20 min at 30°C with 4 mM amounts of each of the nucleotides or nucleotide analogs indicated. Poorly hydrolyzable or nonhydrolyzable analogues such as AMP-PNP, AMP-PCP, and ATP γS do not support ^{55}Fe accumulation. The results shown are the means of triplicate determinations \pm S.E. as indicated. This experiment has been repeated two times with similar results.

Substrate (4 mM)	Transport (% ATP)
ATP	100 ± 4.3
GTP	21.3 ± 1.2
CTP	51.8 ± 4.0
TTP	29.3 ± 4.2
ITP	45.4 ± 0.8
AMP-PNP	3.1 ± 1.7
AMP-PCP	1.2 ± 1.5
ATP γS	7.1 ± 3.3

FIG. 1. Transport of ^{55}Fe in microsomes is time (A)- and temperature (B)-dependent. A, time dependence of iron accumulation in spleen microsomes, (Δ , -ATP; \blacktriangle , +4 mM ATP). Microsomes were prepared as described under "Experimental Procedures" and incubated in the presence of ^{55}Fe for the indicated times. Then, microsomes were collected by rapid filtration and the associated ^{55}Fe determined by liquid scintillation spectrometry. B, temperature dependence of iron accumulation. Temperature dependence of iron accumulation was measured after 20 min of incubation using spleen microsomes as in A and as described under "Experimental Procedures." For both A and B the data shown are the means of triplicate determinations with S.E. as indicated by the error bars. In some cases, the error bars are contained within the symbols. These experiments have been repeated at least five times with similar results.



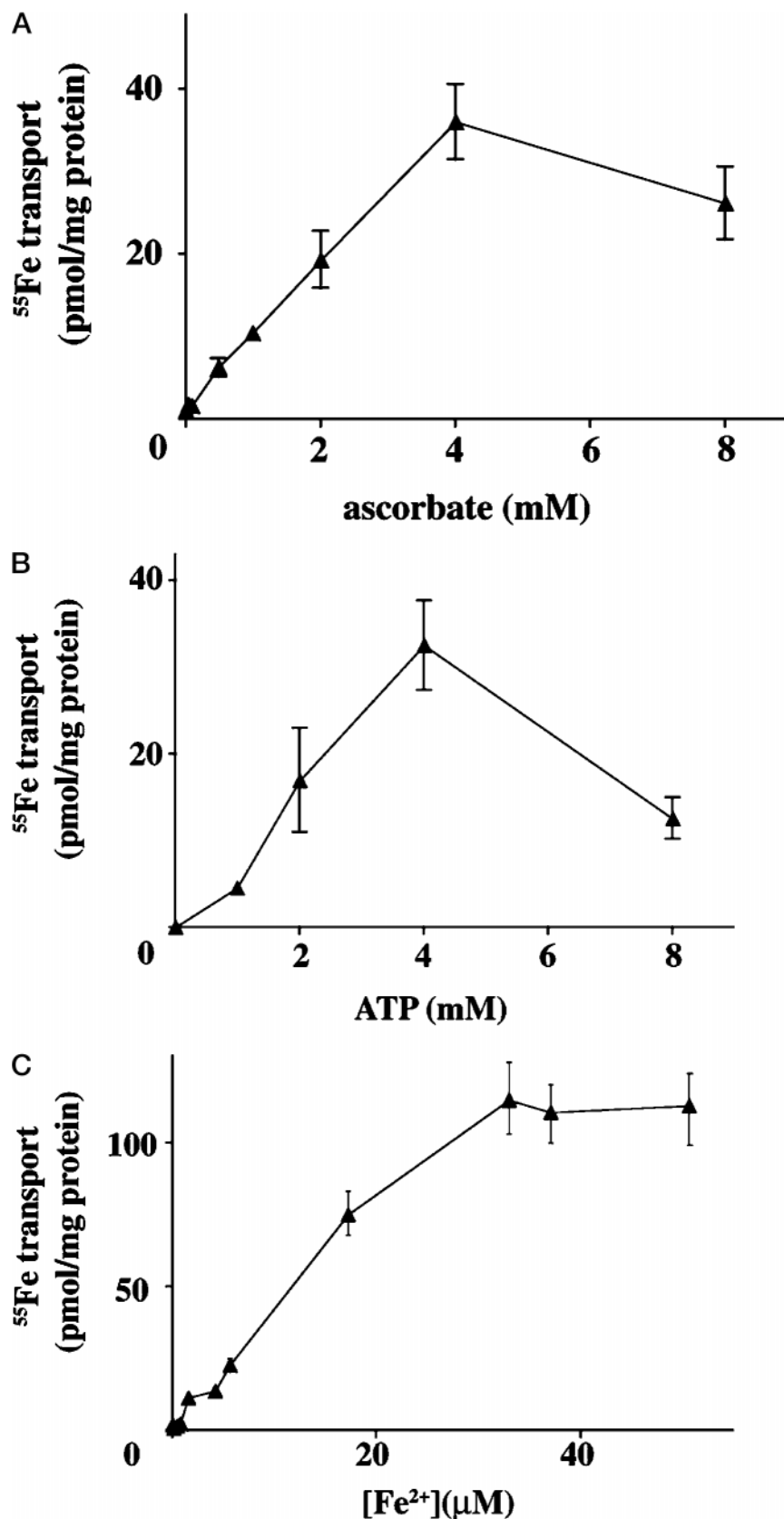


FIG. 2. Transport of ^{55}Fe in microsomes depends on ascorbate (A), ATP (B), and iron (C). A, ascorbate dependence of iron accumulation. Microsomes were prepared as described under "Experimental Procedures" and incubated for 20 min at 30 °C in the presence various of concentrations of ascorbate as indicated. B, ATP dependence of iron accumulation. Spleen microsomes were incubated as described in the legend to A with the indicated concentrations of ATP. C, iron dependence of iron accumulation. Spleen microsomes were incubated as described in the legends to A and B with the indicated concentrations of ^{55}Fe . For all of these experiments the data shown are the means of duplicate or triplicate determinations with S.E. as indicated by the error bars. These experiments has been repeated at least five times with similar results.

in our laboratory. Specific polyclonal antibodies to HO1 and HO2 were generated using recombinant proteins, prepared in *Escherichia coli*, as antigens. Briefly, cDNAs for human HO1 and HO2 were obtained by polymerase chain reaction using human liver cDNA (CLONTECH) as template. Then, human HO1 and HO2 cDNAs were subcloned into pGEX4T2 (Amersham Pharmacia Biotech), and the sequence was confirmed. Next, glutathione *S*-transferase-HO1 and glutathione *S*-trans-

ferase-HO2 were obtained following transformation of competent *E. coli* and purification of the fusion proteins using GSH-Sepharose (Amersham Pharmacia Biotech). The purified antigens were provided for injection into rabbits (Covance, Denver, PA), and the resulting sera were analyzed for specific antibodies. For routine studies, protein samples were fractionated using standard SDS-polyacrylamide gel electrophoresis and transferred to polyvinylidene difluoride membranes. Fol-

lowing incubation in blocking buffer (PBS, 0.1% Tween, 5% nonfat dry milk), blots were incubated in blocking buffer supplemented with either anti-HO1 (1:2500) or anti-HO2 (1:10,000) for 1–18 h. After washing, the blots were incubated with secondary antibody (goat anti-rabbit IgG, 1:5000, Amersham Pharmacia Biotech) for 1 h and developed using chemiluminescence (Renaissance, NEN Life Science Products). Antibody specificity was confirmed by determining the molecular weight of candidate immunoreactive bands and examining tissues derived from mice with genomic deletions of HO1 and HO2 (11, 15). Specific antisera for HO1 and HO2 were obtained without evidence of cross-reacting proteins (data not shown).

Induction of Rhabdomyolysis—Rhabdomyolysis was induced in rats as described previously (16). Briefly, adult male Harlan Sprague-Dawley rats were injected with 7.5 ml/kg glycerol (50% w/v in sterile water) into the anterior thigh muscles. Sham-treated animals were injected with the same volume of saline. After 72 h, rats were sacrificed, and kidney microsomes were prepared for determination of ATP-dependent iron transport and Western blot analysis of HO1 expression as described above.

RESULTS

Identification and Characterization of an Fe-ATPase—To identify a possible iron transporter, we employed ^{55}Fe in attempts to measure ATP-dependent transport of iron into microsomal fractions from rat spleen. In initial experiments, we used rapid filtration onto nitrocellulose filters to monitor the

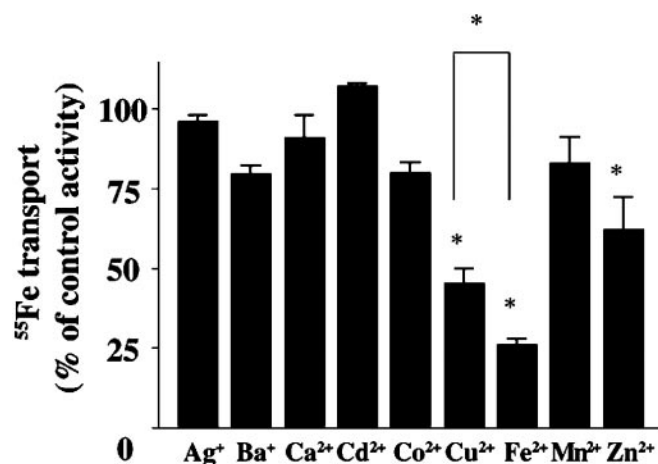
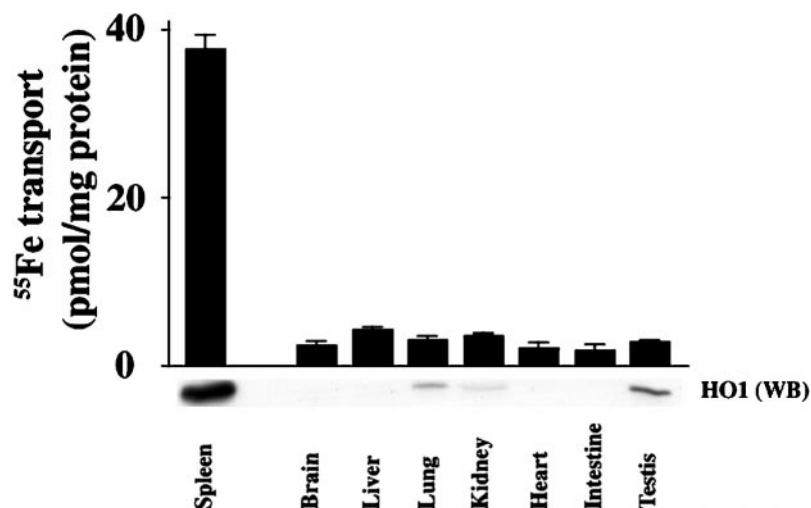


FIG. 3. ^{55}Fe transport in microsomes is specific. Spleen microsomes were prepared as described under “Experimental Procedures” and incubated for 20 min at 30 °C in the presence of 100 μM amounts of various cations as indicated. Statistical significance ($p < 0.0001$) is indicated by the asterisk symbol. The data shown are the means of duplicate or triplicate determinations with S.E. as indicated by the error bars. This experiment has been repeated three times with similar results.

ATP-dependent iron transport and HO1 are co-distributed in tissues. The tissue distribution of HO1 was assessed by Western blot analysis. The tissue distribution of ATP-dependent iron transport was determined as described under “Experimental Procedures” by incubating microsomes derived from the indicated tissues for 20 min at 30 °C. The data shown are the means of triplicate determinations with S.E. as indicated by the error bars. This experiment has been repeated three times with similar results.



^{55}Fe associated with microsomal fractions following various incubation times (see “Experimental Procedures”). These initial experiments were conducted in buffer containing magnesium and potassium chloride, conditions similar to those used for monitoring $^{45}\text{Ca}^{2+}$ accumulation (17, 18). Under these conditions, nearly 80% of added ^{55}Fe was trapped on the filters, and the addition of ATP did not increase apparent ^{55}Fe accumulation. $^{55}\text{FeCl}_3$ is poorly soluble and, in the presence of oxygen, is rapidly converted to $\text{Fe}(\text{OH})_3$, which forms large insoluble complexes (3, 19). Thus, we reasoned that, in the presence of KCl, the ^{55}Fe associated with the filters may represent nonspecific iron precipitates, perhaps $\text{Fe}(\text{OH})_3$ complexes. Accordingly, we replaced KCl with potassium gluconate to avoid iron precipitation. In potassium gluconate buffer, ^{55}Fe associated with the filters was dramatically reduced, indicating that iron did not precipitate. Yet, ATP failed to augment ^{55}Fe accumulation. Since ferrous iron (Fe^{2+}) is the intracellular form of iron in cells (3, 20), we reasoned that a microsomal Fe-ATPase may require iron in the reduced form. Thus, we added ascorbate to the assay buffer, which reduces iron to the ferrous form. Under these conditions ATP stimulates apparent ^{55}Fe transport. Since ATP requiring transporters often use ATP complexed with magnesium ion as a substrate, Mg^{2+} was included for these initial measurements. Omitting Mg^{2+} eliminates the effect of ATP on ^{55}Fe accumulation suggesting that Mg-ATP is required for apparent iron transport.

Conceivably, ATP may increase ^{55}Fe binding to proteins rather than stimulate transmembrane ^{55}Fe transport. However, ATP failed to increase ^{55}Fe associated with cytoplasmic protein fractions or Triton X-100-solubilized microsomal membrane protein preparations (data not shown). If the apparent ATP-dependent ^{55}Fe accumulation is due to an ATP-dependent transporter, then hydrolyzable nucleotide triphosphates should support iron accumulation, while nonhydrolyzable analogues should not. ATP γS , AMP-PCP, and AMP-PNP, which are poorly hydrolyzed, provide <10% of the activity of ATP (Table I). CTP, ITP, and GTP partially support iron accumulation (Table I). If the ^{55}Fe accumulation reflects a membrane transporter rather than ATP-dependent ^{55}Fe binding, it should have time and temperature dependence. ^{55}Fe transport is time-dependent, with linear ^{55}Fe accumulation for about 45 min at 30° (Fig. 1A). ^{55}Fe transport is also temperature-dependent with maximal activity at 37 °C and a Q_{10} of 2.8 between 20 and 30 °C (Fig. 1B). Thus, the ATP-dependent ^{55}Fe accumulation in microsomes does not simply reflect ATP-mediated binding of ^{55}Fe to proteins. The requirement for hydrolyzable high energy phosphate bonds, and the magnesium, time and temperature

dependence, suggest that an ATPase mediates ^{55}Fe transport across microsomal membranes.

As mentioned, in initial experiments, we found that ^{55}Fe transport is dependent upon ascorbate. We characterized the ascorbate requirement of ^{55}Fe transport and found maximal activity at 4 mM ascorbate (Fig. 2A). In addition, we examined the ATP and iron dependence. ^{55}Fe transport occurs at physiological concentrations of ATP with maximal stimulation at 4 mM

TABLE II
Effects of pharmacological inhibitors of ATPases on ATP-dependent iron transport

Spleen microsomes were prepared as described under "Experimental Procedures," and ATP-dependent iron transport was determined following incubation with ^{55}Fe for 20 min at 30 °C with each of the ATPase inhibitors as indicated. Inhibition of ATP-dependent iron transport by orthovanadate is consistent with the Fe-ATPase being a member of the P-type ATPase family. The results shown are the means of triplicate determinations \pm S.E. as indicated. This experiment has been repeated two times with similar results.

Inhibitor	Control activity
	%
Thapsigargin (1 μM)	93.7 \pm 2.1
Bafilomycin (0.2 μM)	94.1 \pm 3.8
Ouabain (1 μM)	90.3 \pm 4.1
Oligomycin (1 μM)	104 \pm 8.2
Orthovanadate (100 μM)	35.1 \pm 2.3

ATP and a decline in apparent transport at higher concentrations (Fig. 2B). ^{55}Fe transport is saturable with half-maximal transport at about 10 μM iron (Fig. 2C). To evaluate whether ^{55}Fe transport activity is specific, we examined a variety of cations (Fig. 3). Minimal effects are observed with 0.1 mM barium, cadmium, calcium, cobalt, or manganese. Zinc ions produce 23% inhibition, while copper(II) inhibits transport about 70%.

To determine whether the ^{55}Fe transport reflects the activity of known ATPases, we evaluated a variety of ATPase-specific pharmacological agents (Table II). Thapsigargin, a potent inhibitor of microsomal Ca^{2+} -ATPases, fails to block ^{55}Fe transport. Bafilomycin, a selective high affinity inhibitor of the V-type ATPases, is similarly ineffective. Oligomycin and ouabain, inhibitors of the mitochondrial proton ATPase and the plasma membrane Na^+/K^+ -ATPase, respectively, are also inactive. Orthovanadate, a known inhibitor of P-type ATPases, reduces ^{55}Fe transport by 65%. Thus, the iron transport activity appears to represent a novel ATP-dependent transport process with the properties of a P-type ATPase.

Localization of the Fe-ATPase—Most of heme and iron turnover occurs in the reticuloendothelial system, primarily the macrophages of the spleen, where senescent red blood cells are phagocytosed, and the iron from the heme in hemoglobin is freed for re-utilization (3). We monitored ^{55}Fe transport in

FIG. 5. Iron-mediated induction of ATP-dependent iron transport in RAW 264.7 cells is biphasic (A) with inhibition of the late phase induction by cycloheximide and actinomycin D (B). A, time dependence of Fe-ATPase induction by FeSO_4 . RAW 264.7 cells were cultured as described under "Experimental Procedures" and incubated with 0.5 mM FeSO_4 for the indicated times prior to preparation of microsomes from the cells. B, inhibition of iron-mediated induction of Fe-ATPase by cycloheximide (CHX) and actinomycin D (AD). RAW 264.7 cells were incubated with 0.5 mM FeSO_4 for 2 or 20 h as indicated. To examine the rapid phase induction, CHX (100 $\mu\text{g}/\text{ml}$) and AD (1 $\mu\text{g}/\text{ml}$) were added 30 min prior to the addition of FeSO_4 , and cells were harvested after 2 h of iron treatment. To study the late phase induction AD was added 30 min prior to the addition of iron, while CHX was withheld due to its toxicity and added 16 h after initiating incubation with 0.5 mM FeSO_4 prior to harvesting the cells after 20 h of iron treatment. The data shown are the means of duplicate or triplicate determinations with standard error as indicated by the error bars. This experiment has been repeated two times with similar results.

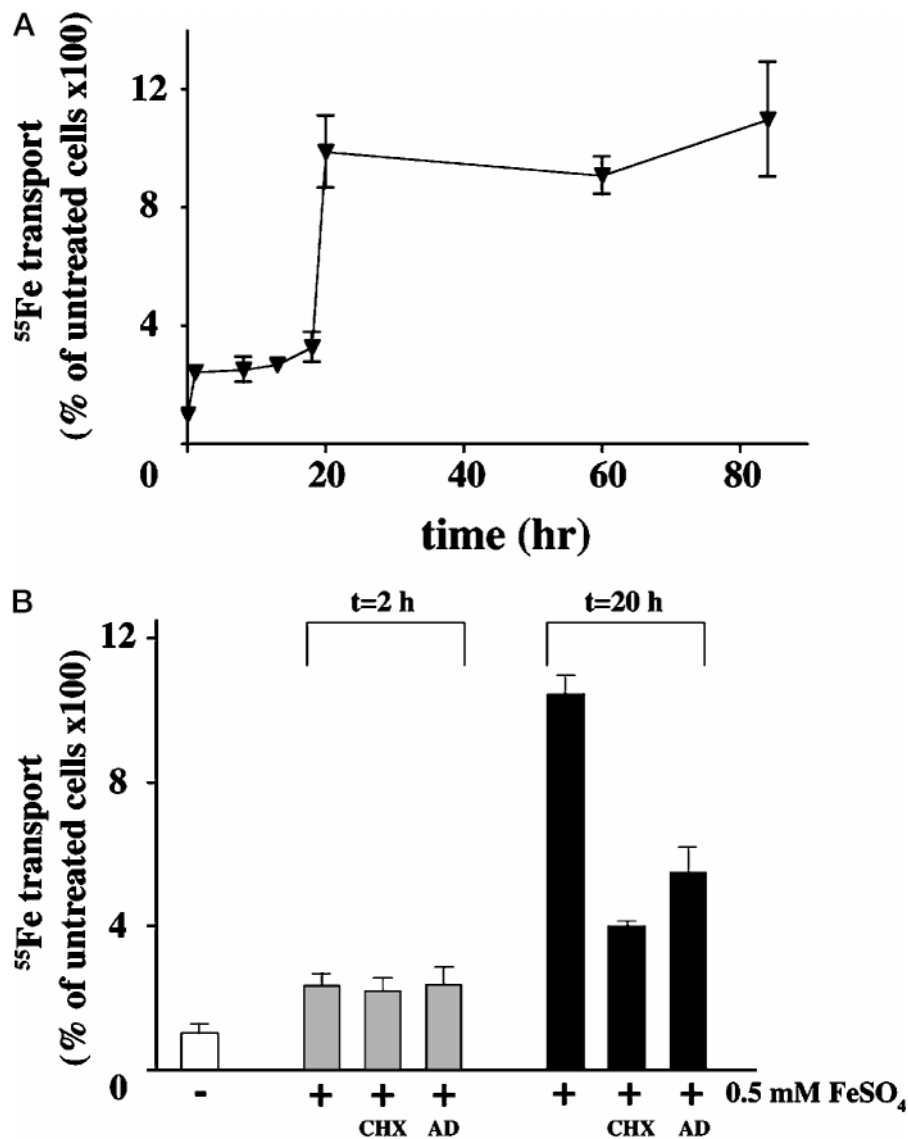
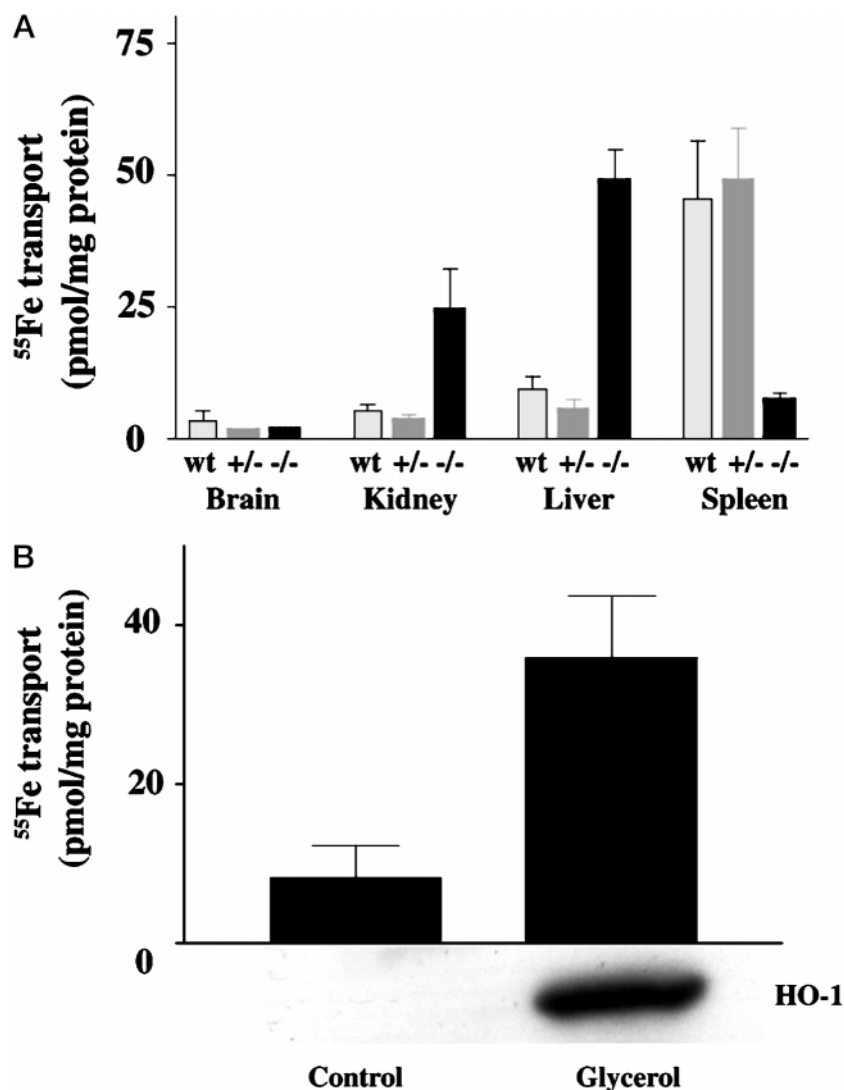


TABLE III
Subcellular distribution of ATP-dependent iron transport

Spleen tissue was homogenized and fractionated as described under "Experimental Procedures." Subcellular fractions were used to determine ATP-dependent iron transport and marker enzyme activity as indicated. The fraction of the total membrane-associated activity recovered for P1, P2, and P3 is indicated in parentheses. The distribution of HO1 was determined by Western blot analysis. In some cases a given enzymatic activity was not detectable as indicated by ND. The biochemical measurements were in duplicate or triplicate. This experiment has been replicated with the same results.

	Cytochrome <i>c</i> oxidase	Alkaline phosphatase	NADPH cytochrome <i>c</i> reductase	HO1 (Western blot)	⁵⁵ Fe transport
	A/min/μg	A/min/mg	A/min/mg		pmol/mg
P1	2.9 ± 0.8 (7%)	0.12 ± 0.03 (20%)	ND	+	ND
P2	32.8 ± 5.1 (77%)	0.10 ± 0.03 (17%)	0.057 ± 0.012 (17%)	+	27.7 ± 0.5 (24%)
P3	6.8 ± 1.0 (16%)	0.36 ± 0.04 (62%)	0.280 ± 0.022 (83%)	+++	88.0 ± 1.8 (76%)

FIG. 6. ATP-dependent iron transport is regulated by iron accumulation in tissues from *HO1*^{-/-} mice (A) and in the kidney in response to glycerol-mediated rhabdomyolysis (B). A, iron-mediated increase in ATP-dependent iron transport in *HO1*^{-/-} mice. Microsomes were prepared from the brain, liver, kidney, or spleen of 40-week-old *HO1*^{-/-}, *HO1*^{+/-}, or wild-type mice, and ATP-dependent iron transport was determined as described under "Experimental Procedures." The data shown are the means of duplicate or triplicate determinations with S.E. as indicated by the error bars. This experiment has been repeated three times with similar results. B, increase in ATP-dependent iron transport in association with induction of HO1 by rhabdomyolysis in rat kidney. Rhabdomyolysis was induced by glycerol injection into skeletal muscle of adult male rats as described under "Experimental Procedures." After 72 h, microsomes were prepared from the kidneys of glycerol and sham-injected animals and ATP-dependent iron transport and HO1 induction (Western blot) were determined. The data shown are the means of duplicate or triplicate determinations with S.E. as indicated by the error bars. This experiment has been repeated three times with similar results.



microsomal fractions from a wide range of rat tissues (Fig. 4). ATP-dependent iron transport is highest in the spleen, almost 20 times higher than levels in any of the other tissues examined. Levels of ATP-dependent iron transport are similar in brain, lung, kidney, heart, intestine, testes, and liver. The high level of ⁵⁵Fe transport in the spleen is paralleled by a comparable enrichment of HO1 protein (Fig. 4). In contrast, HO2 is distributed much differently with selective enrichment in the brain and testes (data not shown).

Since HO1 and ATP-dependent iron transport are co-distributed in tissues, we wondered whether they would have a similar subcellular localization. We conducted limited subcellular fractionation of spleen tissue (Table III). The microsome-enriched fraction (P3) contains >75% of total ⁵⁵Fe transport ac-

tivity. NADPH cytochrome *c* reductase activity, a marker for endoplasmic reticulum, is similarly enriched in the microsomal fraction (P3). Alkaline phosphatase, a enzyme marker for plasma membranes, is also enriched in the microsomal fraction, although the distribution of the ATP-dependent iron transport more closely matches that of NADPH cytochrome C reductase. The nuclear fraction (P1) contains >95% of detectable DNA, yet displays undetectable iron transport. As reported previously (21, 22), HO1 protein is comparably enriched in the microsomal fraction. The mitochondrial protein, cytochrome C oxidase, is concentrated 4–5-fold in P2. The proportion of ATP-dependent iron transport in P2 is similar to that of the endoplasmic reticulum marker (NADPH cytochrome *c* reductase). These findings are consistent with a localization of

the Fe-ATPase in endoplasmic reticulum membranes, together with HO1.

Fe-ATPase Induction by Iron Treatment—The catabolism of hemoglobin heme by HO1 to liberate iron in the spleen takes place in macrophages, which express HO1 whose activity is induced in response to hemin or erythrocytes (23, 24). Accordingly, we examined ^{55}Fe transport in RAW 264.7 cells, a mouse-derived macrophage cell line. Saturable, ATP-dependent, iron transport is readily demonstrable in microsomal fractions of these cells (data not shown). Incubating these cells overnight with 0.5 mM FeSO_4 elicits a 10-fold increase in iron transport (Fig. 5A), while treatment with 0.1 mM FeSO_4 produces a significant but smaller increase (data not shown). The augmented iron transport does not reflect an immediate effect of iron, as incubation of the cells with 0.5 mM iron just prior to homogenization has no effect on iron transport (data not shown). We examined the time dependence for induction of the ATP-dependent iron transport by exogenous iron. We observe a biphasic induction with a 2-fold increase in the first 1–2 h, followed by a plateau, and then a delayed and rapid five-fold induction after 18 h of iron treatment. To address the possible mechanism of iron's induction of ATP-dependent iron transport in RAW 264.7 cells, we examined the effects of transcriptional and translational inhibitors. Inhibition of transcription with actinomycin D (AD), or translation with cycloheximide (CHX), does not block the initial 2-fold induction seen after 1–2 h of iron treatment (Fig. 5B). However, AD and CHX do prevent the delayed induction, reducing the observed iron transport to levels similar to that seen after 2 h of iron treatment (Fig. 5B).

To ascertain the influence of increased iron in intact animals on the ATP-dependent iron transport, we utilized $\text{HO1}^{-/-}$ mice in which accumulation of non-heme iron has been demonstrated (11, 12). ATP-dependent iron transport in kidney microsomes from 40-week-old $\text{HO1}^{-/-}$ mice is increased 5–8-fold compared with levels in heterozygotes that are similar to wild-type specimens (Fig. 6A). In liver microsomes from 40-week-old $\text{HO1}^{-/-}$ mice, the ATP-dependent iron transport is increased >10-fold. The elevated ATP-dependent iron transport is likely due to increased tissue iron levels, since we do not detect an increase in iron transport in microsomes from the kidney and liver of young (10-week-old) $\text{HO1}^{-/-}$ mice whose tissue iron levels are not yet elevated (11) (data not shown). ATP-dependent iron transport in brain microsomes is not increased even in 40-week-old $\text{HO1}^{-/-}$ animals, presumably because iron does not accumulate in the brains of the mutant mice (11) (Fig. 6A). In contrast to the marked augmentation of ATP-dependent iron transport in kidney and liver of $\text{HO1}^{-/-}$ animals, microsomes from the spleen of $\text{HO1}^{-/-}$ mice display a >75% decline in ^{55}Fe transport compared with heterozygote and wild-type specimens (Fig. 6A).

We reasoned that directly elevating cellular iron levels by increasing heme oxygenase activity in tissues might also induce ATP-dependent iron transport. Injection of glycerol into skeletal muscles of rodents causes rhabdomyolysis leading to the release of myoglobin, and its heme, into the circulation. Heme accumulation in the kidney induces HO1, which releases iron from heme (16, 25). Three days after glycerol treatment, we observe a dramatic increase of HO1 protein in the kidney (Fig. 6B). Concurrently, we observe a 5-fold augmentation of ATP-dependent iron transport in kidney microsomes from glycerol treated animals (Fig. 6B).

DISCUSSION

In the present study we report the identification and characterization an Fe-ATPase in mammalian tissues. The iron transport we observe appears to be mediated by an Fe-ATPase, since it is dependent upon hydrolyzable nucleotide triphos-

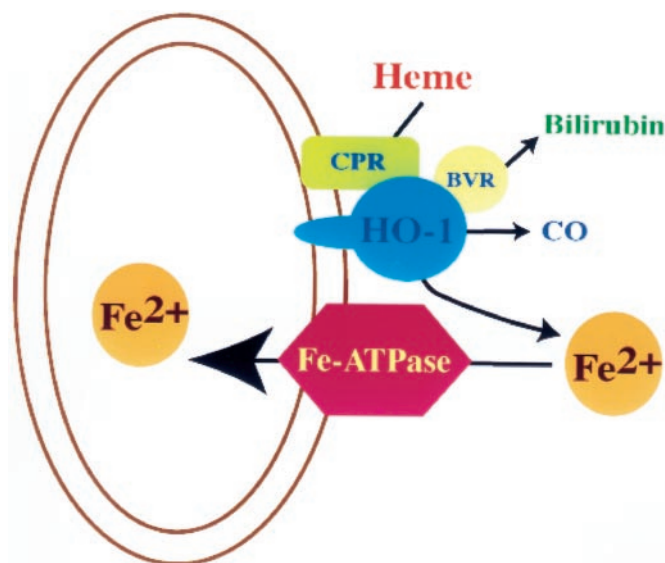


FIG. 7. ATP-dependent iron transport and HO1 are functionally coupled. HO1 is present on the endoplasmic reticulum (ER) membrane, where in conjunction with cytochrome P450 reductase (CPR) and biliverdin reductase (BVR), it catabolizes heme producing bilirubin, carbon monoxide, and Fe^{2+} . Released iron is transiently part of the labile or intermediate iron pool (3) before being transported to the luminal side of the ER by the Fe-ATPase. This fraction of the ER may also include transferrin and transferrin receptors as they are being recycled through the ER compartment back to the plasma membrane through exocytosis. Conceivably, within the lumen of the ER, Fe^{2+} may be oxidized to Fe^{3+} , bind transferrin, and be returned to the extracellular fluid with transferrin following exocytosis.

phates, magnesium, time, and temperature. Inhibition by orthovanadate suggests that the Fe-ATPase may be a P-type ATPase, mediating transmembrane transport through a mechanism that involves transient phosphorylation of an aspartate residue (26–28). The Fe-ATPase we describe appears to be a novel entity, as its activity is not affected by specific inhibitors of the other known ATPases. Conceivably, the ATP-dependent iron transport may reflect transport mediated by a copper ATPase encoded by the Wilson's or Menkes' disease genes (29). However, neither of these genes are significantly expressed in the spleen (30, 31). Meneghini and associates (32) have described nuclear transport of iron in the liver that differs from the Fe-ATPase described here. The transporter they identified utilizes the ferric form of iron (32), which does not support the ATP-dependent iron transport described in this report. Moreover, under our experimental conditions, we do not detect any iron transport in nuclear fractions. Thus, the Fe-ATPase described herein represents a new mammalian transport mechanism.

The total transport activity of the Fe-ATPase is less than that of other P-type ATPases. We measured about 10 pmol/min/mg protein in the spleen, whereas the Ca-ATPase is substantially more active with activities of 115 protein and 234 nmol/min/mg protein in platelet and cerebellar membranes respectively (33). The copper ATPases are the only other metal transporting P-type ATPases described in mammals and direct biochemical measurements of their activity are lacking. While ATP-dependent iron transport is low, this may reflect the low levels of free iron compared with other ions in cells.

Our findings suggest that the ATP-dependent iron transport we have described physiologically regulates cellular iron homeostasis. RAW 264.7 cells manifest significantly augmented ATP-dependent iron transport when treated with iron. In $\text{HO1}^{-/-}$ mice, wherein iron accumulates in the liver and kidney, ATP-dependent iron transport is strikingly augmented. In the

spleen of these mice there is a dramatic reduction in ATP-dependent iron transport, possibly as a result of anemia in these mice (11) leading to a decrease in total erythrocyte turnover. Glycerol-induced rhabdomyolysis, which leads to increased heme levels, HO1 induction, and iron liberation in the kidney, concurrently induces ATP-dependent iron transport. Thus, in cultured cells and animal models, cellular iron accumulation is associated with elevations in ATP-dependent iron transport, implying that, physiologically, the Fe-ATPase responds to iron.

Our findings suggest that the regulatory mechanisms determining expression and induction of ATP-dependent iron transport may be complex. We observe a biphasic induction of ATP-dependent iron transport in RAW 264.7 cells that may reflect different underlying mechanisms. Rapid induction (1–2 h following treatment with iron) may reflect post-translational modifications as the initial induction is not blocked by CHX or AD. A more pronounced induction 16–20 h after iron treatment is blocked by incubation with CHX and AD. Even when added to the cells 16 h after the iron, CHX blocks the delayed induction. Other genes related to cellular iron homeostasis, such as transferrin receptor and ferritin, are regulated by IRPs (4, 6, 34). Thus, with iron deficiency, IRPs prevent the translation of ferritin mRNA and stabilize transferrin receptor mRNA. IRPs also regulate the heme-synthesizing enzyme Δ -aminolevulinic synthase as well as the divalent cation transporter-1 (5, 35, 36). Our results suggest that a rapid, perhaps post-translational, regulatory mechanism mediates the 2-fold induction of ATP-dependent iron transport seen in the first 1–2 h, and a second, translational (*e.g.* IRE-mediated) or transcriptional regulatory mechanism underlies the delayed induction of ATP-dependent iron transport after 18 h of iron exposure. Since both CHX and AD block iron-mediated induction of ATP-dependent iron transport, we cannot exclude an IRE-mediated mechanism.

A variety of evidence suggests that HO1 is functionally coupled to the Fe-ATPase and iron mobilization (11, 12). HO1 transfection stimulates iron egress from cells, which is markedly diminished in cells from *HO1*^{-/-} mice (12). The ATP-dependent iron transport is more than 20-fold enriched in spleen compared with other tissues, closely resembling the distribution of HO1. Increases in cellular iron, both *in vitro* and *in vivo*, induce HO1 and the Fe-ATPase in parallel. HO1 and the Fe-ATPase are similarly enriched in microsomal fractions, where they may co-localize on endoplasmic reticulum membranes. Accordingly, we suggest that HO1 and the Fe-ATPase act in concert (Fig. 7). As heme is degraded by HO1, the freed iron is transported by the Fe-ATPase to the luminal side of the endoplasmic reticulum for subsequent exocytosis (Fig. 7). Iron may bind transferrin in the lumen of the ER if the pH is neutral or following exocytosis. Transferrin is important for physiologic iron uptake, although alternate pathways enable cells to acquire iron. Interestingly, transferrin may be required for cellular iron release. Thus, in a perfused organ model, transferrin was required for ⁵⁹Fe release from the liver (37). In our own studies, monitoring ⁵⁵Fe release from HEK-293 cells, we find

that cells take up ⁵⁵Fe in the absence of transferrin, although ⁵⁵Fe is released only in the presence of transferrin.² Together these findings suggest that a portion of the endoplasmic reticulum may be devoted to the regulation of iron uptake, heme turnover, and iron efflux with specific roles for transferrin receptor, HO1, and the Fe-ATPase in close association.

REFERENCES

1. Meneghini, R. (1997) *Free Radic. Biol. Med.* **23**, 783–792
2. McCord, J. M. (1998) *Semin. Hematol.* **35**, 5–12
3. Richardson, D. R., and Ponka, P. (1997) *Biochim. Biophys. Acta.* **1331**, 1–40
4. Ponka, P., Beaumont, C., and Richardson, D. R. (1998) *Semin. Hematol.* **35**, 35–54
5. Gunshin, H., Mackenzie, B., Berger, U. V., Gunshin, Y., Romero, M. F., Boron, W. F., Nussberger, S., Gollan, J. L., and Hediger, M. A. (1997) *Nature* **388**, 482–488
6. Hentze, M. W., and Kuhn, L. C. (1996) *Proc. Natl. Acad. Sci. U. S. A.* **93**, 8175–8182
7. Rouault, T. A., and Klausner, R. D. (1996) *Exs* **77**, 183–197
8. Conrad, M. E. (1998) *Semin. Hematol.* **35**, 1–4
9. Maines, M. D. (1997) *Annu. Rev. Pharmacol. Toxicol.* **37**, 517–554
10. Poss, K. D., and Tonegawa, S. (1997) *Proc. Natl. Acad. Sci. U. S. A.* **94**, 10925–10930
11. Poss, K. D., and Tonegawa, S. (1997) *Proc. Natl. Acad. Sci. U. S. A.* **94**, 10919–10924
12. Ferris, C. D., Jaffrey, S. R., Sawa, A., Takahashi, M., Brady, S. D., Barrow, R. K., Tysoe, S. A., Wolosker, H., Barañano, D. E., Dore, S., Poss, K. D., and Snyder, S. H. (1999) *Nat. Cell Biol.* **1**, 152–157
13. Storrie, B., and Madden, E. A. (1990) *Methods Enzymol.* **182**, 203–225
14. Raschke, W. C., Baird, S., Ralph, P., and Nakoinz, I. (1978) *Cell* **15**, 261–267
15. Poss, K. D., Thomas, M. J., Ebralidze, A. K., O'Dell, T. J., and Tonegawa, S. (1995) *Neuron* **15**, 867–873
16. Nath, K. A., Balla, G., Vercellotti, G. M., Balla, J., Jacob, H. S., Levitt, M. D., and Rosenberg, M. E. (1992) *J. Clin. Invest.* **90**, 267–270
17. Supattapone, S., Danoff, S. K., Theibert, A., Joseph, S. K., Steiner, J., and Snyder, S. H. (1988) *Proc. Natl. Acad. Sci. U. S. A.* **85**, 8747–8750
18. Muallem, S., Schoeffield, M., Pandol, S., and Sachs, G. (1985) *Proc. Natl. Acad. Sci. U. S. A.* **82**, 4433–4437
19. Brunner-Dopper, L., Kriegerbeckova, K., Kovar, J., and Goldenberg, H. (1998) *Anal. Biochem.* **261**, 128–130
20. Umbreit, J. N., Conrad, M. E., Moore, E. G., and Latour, L. F. (1998) *Semin. Hematol.* **35**, 13–26
21. Tenhunen, R., Marver, H. S., and Schmid, R. (1968) *Proc. Natl. Acad. Sci. U. S. A.* **61**, 748–755
22. Tenhunen, R., Marver, H. S., and Schmid, R. (1969) *J. Biol. Chem.* **244**, 6388–6394
23. Pimstone, N. R., Tenhunen, R., Seitz, P. T., Marver, H. S., and Schmid, R. (1971) *J. Exp. Med.* **133**, 1264–1281
24. Gemsa, D., Woo, C. H., Fudenberg, H. H., and Schmid, R. (1973) *J. Clin. Invest.* **52**, 812–822
25. Zager, R. A. (1996) *Kidney Int.* **49**, 314–326
26. MacLennan, D. H., Rice, W. J., and Green, N. M. (1997) *J. Biol. Chem.* **272**, 28815–28818
27. Inesi, G., and Kirtley, M. R. (1992) *J. Bioenerg. Biomembr.* **24**, 271–283
28. Moller, J. V., Juul, B., and le Maire, M. (1996) *Biochim. Biophys. Acta* **1286**, 1–51
29. Schaefer, M., and Gitlin, J. D. (1999) *Am. J. Physiol.* **276**, G311–G314
30. Paynter, J. A., Grimes, A., Lockhart, P., and Mercer, J. F. (1994) *FEBS Lett.* **351**, 186–190
31. Bull, P. C., Thomas, G. R., Rommens, J. M., Forbes, J. R., and Cox, D. W. (1993) *Nat. Genet.* **5**, 327–337
32. Gurgueira, S. A., and Meneghini, R. (1996) *J. Biol. Chem.* **271**, 13616–13620
33. Engelder, S., Wolosker, H., and de Meis, L. (1995) *J. Biol. Chem.* **270**, 21050–21055
34. Klausner, R. D., Rouault, T. A., and Harford, J. B. (1993) *Cell* **72**, 19–28
35. Dandekar, T., Stripecke, R., Gray, N. K., Goossen, B., Constable, A., Johansson, H. E., and Hentze, M. W. (1991) *EMBO J.* **10**, 1903–1909
36. Cox, T. C., Bawden, M. J., Martin, A., and May, B. K. (1991) *EMBO J.* **10**, 1891–1902
37. Baker, E., Morton, A. G., and Tavill, A. S. (1980) *Br. J. Haematol.* **45**, 607–620

² C. D. Ferris and S. H. Snyder, unpublished observations.

A Mammalian Iron ATPase Induced by Iron

David E. Barañano, Herman Wolosker, Byoung-Il Bae, Roxanne K. Barrow, Solomon H. Snyder and Christopher D. Ferris

J. Biol. Chem. 2000, 275:15166-15173.

doi: 10.1074/jbc.275.20.15166

Access the most updated version of this article at <http://www.jbc.org/content/275/20/15166>

Alerts:

- [When this article is cited](#)
- [When a correction for this article is posted](#)

[Click here](#) to choose from all of JBC's e-mail alerts

This article cites 35 references, 12 of which can be accessed free at <http://www.jbc.org/content/275/20/15166.full.html#ref-list-1>